12-1-2019

Tricarboxylic acid cycle enzyme activities in a mouse model of methylmalonic aciduria

Parith Wongkittichote

Gary Cunningham

Marshall L Summar

Elena Pumbo

Patrick Forny

See next page for additional authors

Authors

Parith Wongkittichote, Gary Cunningham, Marshall L Summar, Elena Pumbo, Patrick Forny, Matthias R Baumgartner, and Kimberly A Chapman

Molecular Genetics and Metabolism 128 (2019) 444–451

Contents lists available at ScienceDirect

Molecular Genetics and Metabolism

journal homepage: www.elsevier.com/locate/ymgme

Tricarboxylic acid cycle enzyme activities in a mouse model of methylmalonic aciduria

Parith Wongkittichote[a,b,c], Gary Cunningham[a], Marshall L. Summar[a], Elena Pumbo[a], Patrick Forny[d,e], Matthias R. Baumgartner[d,e], Kimberly A. Chapman[a,*]

[a] Children's National Rare Disease Institute, Children's National Health System, Washington DC 20010, United States
[b] Department of Pediatrics, Faculty of Medicine Ramathibodi Hospital, Mahidol University, Bangkok 10400, Thailand
[c] Department of Pediatrics, St. Louis Children's Hospital, Washington University School of Medicine, St. Louis, MO, USA
[d] Division of Metabolism, the Children's Research Center, The Swiss Newborn Screening Laboratory, University Children's Hospital Zurich, 8032 Zurich, Switzerland
[e] The radiz–Rare Disease Initiative Zurich, Clinical Research Priority Program for Rare Diseases, the Center for Integrative Human Physiology, University of Zurich, 8006 Zurich, Switzerland

ARTICLE INFO

Keywords:
Methylmalonic aciduria
Tricarboxylic acid cycle
Citric acid cycle
Mitochondria
TCA cycle
Anaplerosis
Energy metabolism

ABSTRACT

Methylmalonic acidemia (MMA) is a propionate pathway disorder caused by dysfunction of the mitochondrial enzyme methylmalonyl-CoA mutase (MMUT). MMUT catalyzes the conversion of methylmalonyl-CoA to succinyl-CoA, an anaplerotic reaction which feeds into the tricarboxylic acid (TCA) cycle. As part of the pathological mechanisms of MMA, previous studies have suggested there is decreased TCA activity due to a "toxic inhibition" of TCA cycle enzymes by MMA related metabolites, in addition to reduced anaplerosis. Here, we have utilized mitochondria isolated from livers of a mouse model of MMA (*Mut*-ko/ki) and their littermate controls (Ki/wt) to examine the amounts and enzyme functions of most of the TCA cycle enzymes. We have performed mRNA quantification, protein semi-quantitation, and enzyme activity quantification for TCA cycle enzymes in these samples. Expression profiling showed increased mRNA levels of fumarate hydratase in the *Mut*-ko/ki samples, which by contrast had reduced protein levels as detected by immunoblot, while all other mRNA levels were unaltered. Immunoblotting also revealed decreased protein levels of 2-oxoglutarate dehydrogenase and malate dehydrogenase 2. Interesting, the decreased protein amount of 2-oxoglutarate dehydrogenase was reflected in decreased activity for this enzyme while there is a trend towards decreased activity of fumarate hydratase and malate dehydrogenase 2. Citrate synthase, isocitrate dehydrogenase 2/3, succinyl-CoA synthase, and succinate dehydrogenase are not statistically different in terms of quantity of enzyme or activity. Finally, we found decreased activity when examining the function of methylmalonyl-CoA mutase in series with succinate synthase and succinate dehydrogenase in the *Mut*-ko/ki mice compared to their littermate controls, as expected. This study demonstrates decreased activity of certain TCA cycle enzymes and by corollary decreased TCA cycle function, but it supports decreased protein quantity rather than "toxic inhibition" as the underlying mechanism of action.

Summary: Methylmalonic acidemia (MMA) is an inborn metabolic disorder of propionate catabolism. In this disorder, toxic metabolites are considered to be the major pathogenic mechanism for acute and long-term complications. However, despite optimized therapies aimed at reducing metabolite levels, patients continue to suffer from late complications, including metabolic stroke and renal insufficiency. Since the propionate pathway feeds into the tricarboxylic acid (TCA) cycle, we investigated TCA cycle function in a constitutive MMA mouse model. We demonstrated decreased amounts of the TCA enzymes, Mdh2 and Ogdh as semi-quantified by immunoblot. Enzymatic activity of Ogdh is also decreased in the MMA mouse model compared to controls. Thus, when the enzyme amounts are decreased, we see the enzymatic activity also decreased to a similar extent for Ogdh. Further studies to elucidate the structural and/or functional links between the TCA cycle and propionate pathways might lead to new treatment approaches for MMA patients.

* Corresponding author at: 111 Michigan Ave, NW, Washington DC 20010, USA.
E-mail address: KChapman@childrensnational.org (K.A. Chapman).

https://doi.org/10.1016/j.ymgme.2019.10.007
Received 12 July 2019; Received in revised form 19 September 2019; Accepted 15 October 2019
Available online 17 October 2019

1. Introduction

Isolated methylmalonic acidemia (MMA, OMIM #251000, 251100, 251110) is a severe inborn error of metabolism caused by dysfunction of the propionate pathway, involved in the catabolism of odd-chain fatty acids, valine, isoleucine, methionine, threonine, and cholesterol to succinyl-CoA, which is subsequently metabolized in the tricarboxylic acid (TCA) cycle. Isolated MMA is characterized by a defect in conversion of (D-)methylmalonyl-CoA to succinyl-CoA, due to deficiency of the methylmalonyl-CoA mutase (MMUT) enzyme (E.C. 5.4.99.2), and may be caused by mutations in the *MMUT* gene, mutations in genes involved in production of its cofactor adenosyl-cobalamin, or mutations in *MCEE* (E.C. 5.1.99.1) or succinate synthetase (*SUCLG1/SUCLA2*), enzymes directly proximal and distal to MMUT [1,2] (Fig. 1). The patients who suffer from MMA can present in the neonatal period with coma and metabolic crisis (including severe metabolic acidosis and hyperammonemia), and if left untreated, die within the first few days of life [3,4].

With the establishment of newborn screening, MMA patients can be detected early and pre-symptomatic treatment can be achieved. However, despite early intervention, long-term complications are observed in these patients [5,6], including neurologic and neurodevelopmental abnormalities [2,7,8]. Renal insufficiency is also common among MMA patients and this might lead to end-stage renal disease [7,9]. The pathophysiology of these late complications is yet to be elucidated. Previous studies found abnormalities in various metabolic pathways, such as the electron transport system in mitochondria [10–12] and amino acid metabolism [13,14]. Mitochondrial dysfunction and oxidative stress were observed in patients with MMA and was thought to play important roles in the development of renal complications [15,16]. Two prominent mechanisms proposed to explain the long-term complications of MMA include 1) the concept of "toxic metabolites" derived from accumulation of methylmalonyl-CoA and propionyl-CoA excess interrupting, among other things, TCA enzyme function [17] and the urea cycle [18] and 2) shortage of TCA cycle intermediates. Propionyl-CoA itself has been shown to inhibit pyruvate dehydrogenase complex (PDHc) activity [10], while 2-methylcitrate, formed by a condensation reaction of propionyl-CoA and oxaloacetate, can inhibit various enzymes in the TCA cycle, such as, citrate synthase (CS), isocitrate dehydrogenase (IDH2/3) and the α-ketoglutarate dehydrogenase complex (OGDHc) [19]. In general, the toxic intermediate role in disease pathophysiology predicts abnormalities in dehydrogenase activity due to inhibition from toxins. On the other hand, impaired anaplerosis of the TCA cycle might be due to the decreased production of succinyl-CoA by MMUT in the propionate pathway, as well as by formation of 2-methylcitrate, which reduces availability of oxaloacetate [20,21].

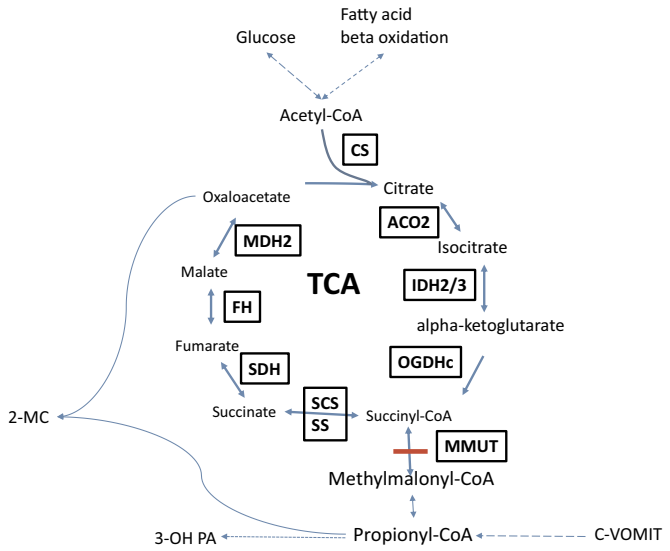

Fig. 1. TCA cycle and Propionate Pathway. A diagram of the TCA cycle showing its intermediates and energy sources. TCA is fed by the propionate pathway, glycolysis and fatty acid oxidation (via acetyl-CoA) which all help to maintain TCA intermediates. The propionate pathway is characterized by production of propionyl-CoA and is involved in metabolism of cholesterol, valine, odd chain fatty acids, methionine, isoleucine and threonine (c-VOMIT). Mut is the last step in the propionate pathway and feeds succinyl-CoA into the TCA cycle. Here, the intermediates and enzymes of interest (boxed and capitalized) are listed. Two known "toxins", 2-methylcitrate and 3-hydroxypropionate are also illustrated. Abbreviations: CS (citrate synthase), aconitase 2 (ACO2), isocitrate dehydrogenase 2/3 (IDH2/3), 2-oxoglutarate dehydrogenase complex (OGDHc), succinate synthase (SS), succinyl-CoA synthetase (SCS), methylmalonyl-CoA mutase (MUT), propionyl-CoA carboxylase (PCC), c-VOMIT (cholesterol, valine, odd chain fatty acids, methionine, isoleucine, threonine), succinate dehydrogenase (SDH), fumarate hydratase (FH), malate dehydrogenase 2 (MDH2), 2-methycitrate (2-MC), 3-hydroxypropionic acid (3-OH PA).

Previously, TCA cycle enzymes have been proposed to work as a complex, called the "metabolon", which allows metabolite channeling [22]. Although more evidence is needed, several studies provide support for the presence of the TCA cycle metabolon [23,24], as well as metabolons involved in other human metabolic pathways, including the initial steps of branched-chain amino acid metabolism [25]. If substrate channeling, created by the interaction of the enzymes which make up a metabolon unit, is necessary for effective metabolism, deficiency in the quantity of one enzyme might affect the function of the others. Since MMUT is a mitochondrial enzyme immediately proximal to the TCA cycle, it may function as part of the TCA cycle metabolon. By this hypothesis, pathological mutations in *Mmut* might affect the structure and/or function of the proposed TCA cycle metabolon and subsequently lead to decreased TCA cycle function.

We have used a mouse model of MMA (*Mut*-ko/ki) which has been described in Forny et al. [26] to model the human disease. These mice are genetic hybrids which carry a knock-out allele of the *Mmut* gene [27] in combination with the knock-in allele p.M698K, corresponding to the human p.M700K mutation [26]. Like the human disease, these mice (*Mut*-ko/ki) demonstrate elevated methylmalonic acid, propionylcarnitine, and 2-methylcitrate, but retain about 1% enzyme activity [26].

Here we demonstrate that the protein levels of OGDH, the TCA cycle enzyme is decreased in *Mut*-ko/ki livers compared to littermate controls, despite a lack of difference in mRNA levels. Several other TCA cycle enzymes protein levels are also decreased and these contribute to decreased specific enzyme and whole pathway activity, as measured in isolated mitochondria. These data support the finding of decreased TCA cycle activity in MMA, but suggest this effect may be due to decreased metabolon function rather than an inhibitory effect of toxic intermediates.

2. Material and methods

2.1. Tissue

Flash frozen livers were taken from methylmalonyl-CoA mutase knock-out/knock-in (*Mut*-ko/ki) mice that have been described in Forny et al. [26]. They are referred to as MMA or *Mut*-ko/ki, here. Littermates, which carry one knock-in and one wild-type allele (and have 50% *Mmut* expression and normal metabolite levels), were used as controls (Ctl or *ki/wt*). Animal experiments were performed in accordance with policies of the Veterinary Office of the State of Zurich and Swiss law on animal protection. Animal studies were approved by the Cantonal Veterinary Office Zurich under license number 202/2014. All mice were sacrificed between 30 and 40 days of life and were predominately females.

2.2. Mitochondrial isolation

Mitochondria from flash frozen livers of Ctl and *Mut*-ko/ki mice were isolated. Briefly, each mouse liver was ground, weighed on ice and placed in 15 mL mitochondrial isolation buffer (5 mM Tris-HCl pH 7.2, 250 mM sucrose and 1 mM EDTA, pH 7.2) and homogenized. The sample was then centrifuged at 484*g* for 10 min at 4° C and the supernatant collected. The supernatant then underwent centrifugation at 9800*g* for 10 min at 4° C and the pellet was collected. The pellet was resuspended in 4 mL and transferred to 2 new tubes. The samples were again centrifuged at 484*g* for 10 min at 4 °C and supernatant collected. The supernatant then underwent centrifugation again at 9800*g* for 10 min at 4 °C. The pellet was collected and resuspended in mitochondrial isolation buffer and centrifuged at 18,000*g* for 5 min at 4° C. The pellet is mitochondria and can be stored at -80° C. The mitochondrial pellet was resuspended in extraction buffer (which opens mitochondria) (5 mM Tris-HCl pH 7.2, 250 mM sucrose, 1 mM EDTA, 1% IDEPAL, 1 tablet Mini protease inhibitor (Roche) per 10 mL, pH to 7.5 with glacial acetic acid) prior to use in every assay. The protein quantification of mitochondria was then performed using Pierce™ BCA Protein Assay Kit (ThermoFisher Scientific).

2.3. Enzymes assay

All TCA enzymes were measured spectrophotometrically (xMark™ Microplate Absorbance Spectrophotometer (Bio-Rad)) using isolated mitochondria. All measures were done in Kinetic mode at 25°C, at the wavelengths described below for each specific assay, with measurements taken every 20 s for at least 30 cycles unless otherwise specified. Each individual enzyme assay was performed in triplicate and the resulting enzyme rates averaged. The rate was determined according to the linear portion of each pattern. Each condition (i.e. *Mut*-ko/ki versus ki/wt ctl) was assayed using three separate samples from three separate animals. Distilled Water (dW) was used as a control substituting for the enzyme substrate for each reaction in the assays shown in Fig. 2. Reaction rates were not corrected for dW rates.

2.4. Citrate synthase (Cs) (E.C. 2.3.3.8)

Cs activity was measured by detecting thiobis(2-nitrobezoic acid) (TNB), a by-product of the reaction between coenzyme A (CoA-SH) and 5,5'dithiobis(2-nitrobenzoic acid) (DTNB) since CoA-SH is released by the reaction (Suppl. Fig. S1. A.). The assay is started when 1 mM oxaloacetate is added to 5 μg of mitochondrial samples mixed with reaction buffer (10 mM tris-HCl pH 8.0, 0.1 mM DTNB, 0.2 mM acetyl Co-A, 0.18% Triton-X). The production of TNB was followed spectrophotometrically at 412 nm as similarly described in Shephard et al. [28] measuring every 20 s for 30 cycles. The results were graphed and slope (which correlates to enzyme rate) was determined. The enzyme activity was then calculated.

2.5. Isocitrate dehydrogenase 2/3 (Idh2/3) (E.C. 1.1.1.41 and 1.1.1.42)

The activity of Idh2/3 was determined by measuring production of NADPH at 340 nm (Suppl. Fig. S2 A). The reaction was started by adding 200 μL of reaction buffer (10 mM potassium phosphate pH 7.4, 2 mM $MgCl_2$, 1 mM NADP and 5 mM isocitrate) to 30 μg of mitochondria [29] and measurements taken every 20 s for 30 cycles. Each analysis was done in triplicate and the resulting slopes averaged and used to determine enzyme activity.

2.6. α-Ketoglutarate dehydrogenase complex (Ogdhc))(E.C. 1.2.4.2)

The reaction mixture containing 63 mM Tris-HCl pH 7.4, 2 mM MgCl2, 0.63 mM potassium-EDTA, 2 mM $CaCl_2$, 1 mM DTT, 0.2 mM TTP, 1 mM NAD +, 0.3 mM coenzyme A, 0.5% Triton-X was added to 30 μg of mitochondria samples. The reaction started by adding 1 mM α-ketoglutaric acid. The production of NADH was measured spectrophotometrically at 340 nm [30] and measurements were taken every 20 s for 30 cycles (Suppl. Fig. S3 A). Each analysis was done in triplicate and the resulting slopes averaged and used to determine enzyme activity.

2.7. Succinyl-CoA synthetase (Scs) (E.C. 6.2.1.5 and 6.2.1.4)

The Scs assay was achieved by Succinyl-CoA Synthetase Activity Colorimetric Assay Kit (BioVision Inc.). The reaction buffer was mixed according to the manufacturer's instructions and 20 μg of mitochondrial samples were added to start the reaction and followed as instructed by the assay kit (Suppl. Fig. S4 A). Each analysis was done in triplicate and the resulting slopes averaged and used to determine enzyme activity.

2.8. Succinate dehydrogenase (Sdh) (E.C. 1.3.5.1)

The activity of Sdh was determined based on its ability to reduce DCPIP, an artificial electron acceptor (Suppl. Fig. S5 A). The reaction mixture of 50 mM potassium phosphate pH 7.4, 0.14 mM DCPIP, 0.1 mM duroquinone, 0.8 mM PMS, 8 uM rotenone, and 12 mM succinate was added to 30 μg of mitochondrial samples. The assay was measured at 600 nm [31,32] every 20 s for 30 cycles. Each analysis was done in triplicate and the resulting slopes averaged and used to determine enzyme activity.

2.9. Fumarate hydratase (Fh)

The reverse reaction of Fh starts with malate and generates fumarate which was detected at OD 250 nm (Suppl. Fig. S6 A). To start the reaction, mitochondria (30 μg) were placed in reaction buffer (50 mM Na_2HPO_4, 0.1% BSA, and 50 mM malic acid). The reaction was followed spectrophotometrically at 250 nm and measurements are taken every 20 s for 30 cycles [33]. Each analysis was done in triplicate and the resulting slopes averaged and used to determine enzyme activity.

2.10. Malate dehydrogenase 2 (Mdh2) (E.C.1.1.1.37)

The reverse function of Mdh2 was measured by following the decrease of NADH at OD 340 nm (Suppl. Fig. S7 A). The reaction mixture contained 100 mM potassium phosphate, 1 mM NADH, and, 2 mM oxaloacetate. The reaction was started by adding 200 μL of reaction mixture to 30 μg of mitochondrial samples [34] and measured at 340 nm every 15 s for 30 cycles. Each analysis was done in triplicate and resulting slopes (correlate with enzyme activity) were averaged.

2.11. Mut-Ss-Sdh coupled assay

Mmut, succinate synthase (Ss) and Sdh were assayed in series in a coupled assay (Suppl. Fig. S10 A). Reaction buffer containing 50 mM potassium phosphate pH 7.4, 10 mM $MgCl_2$, 0.14 mM DCPIP, 0.1 mM duroquinone, 0.8 mM PMS, 8 uM rotenone, 0.01 mM AdoCbl, and 1 mM methylmalonyl-CoA was added to 30 μg of mitochondrial samples. The reduction of DCPIP was followed spectrophotometrically at 600 nm [31,35]). Measurements were taken every 20 s for 30 cycles. The slope of the line created correlates with the serial enzyme activity. Since the measure is from SDH there is residual activity as seen in the control with no methylmalonyl-CoA, but with all the other components of the reaction buffer.

2.12. Immunoblotting

For each sample, 5 μg protein (in mitochondrial lysate) was loaded into an Any kD™ Mini-PROTEAN® (Bio-rad) acrylamide gel. The primary antibodies used for probing each enzyme were anti-Cs (ab96600,

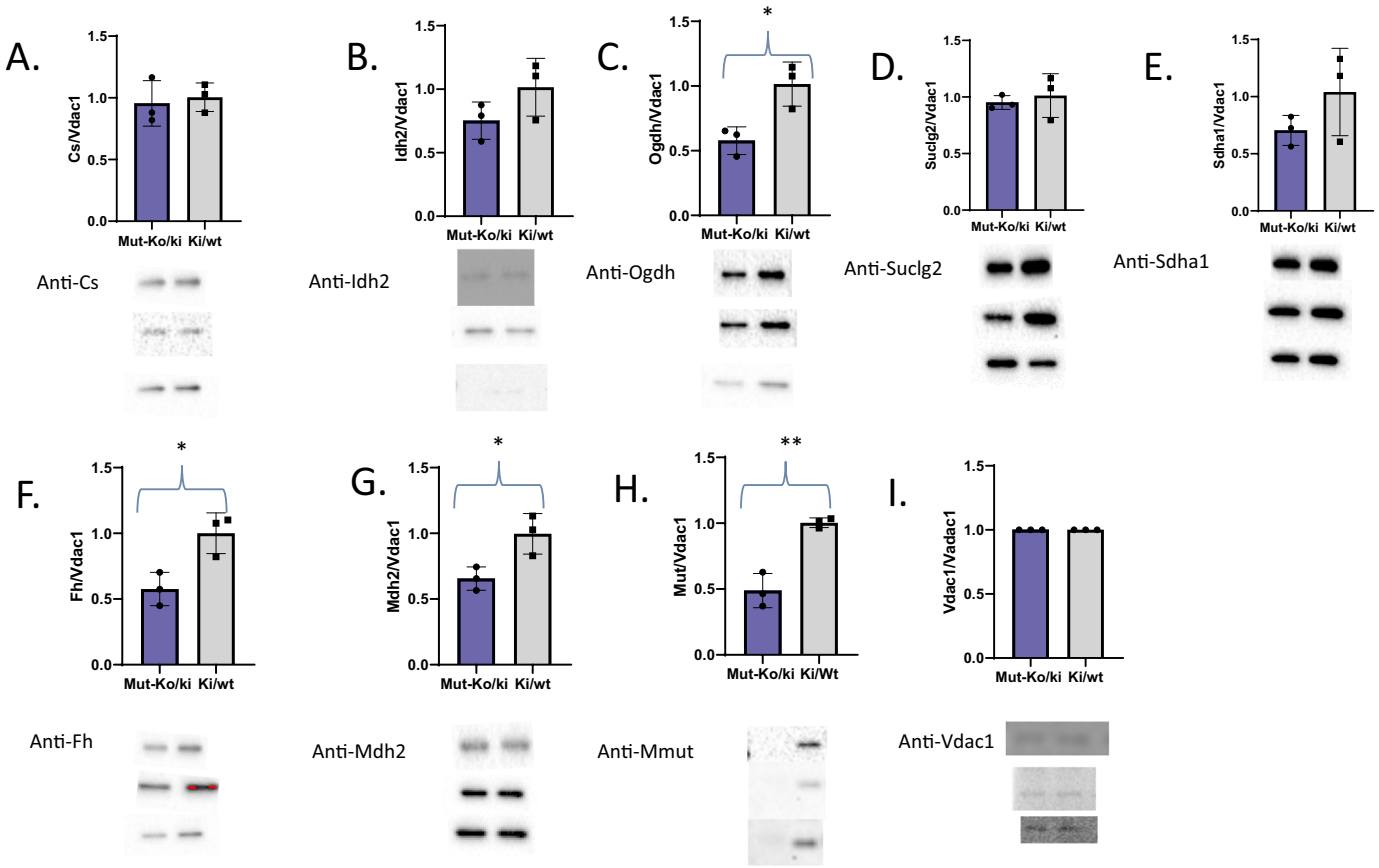

Fig. 2. Immunoblots and quantitation bar graphs of the TCA cycle enzyme amounts from three separate *Mut*-ko/ki mice and three separate Ctl mice. Primary antibody used is listed on the left by each blot. These blots were semi-quantitated using the ChemiDoc™ MP Imaging System (170–8280; Bio-Rad) and Image Lab Software 5.1 by BioRad and listed in Table 3. No manipulation of the original pictures has been done and samples run as *Mut*-ko/ki, Ctl pairs, and then splitting nitrocellulose to probe multiple enzymes at one time. Bar graphs for each quantitation normalized to Vdac1 (blue is *Mut*-ko/ki and grey is Ki/wt). * $p < .05$, **$p < .01$. (For interpretation of the references to colour in this figure legend, the reader is referred to the web version of this article.)

Abcam, 1:5000), anti-Idh2 (ab94359, Abcam, 1:500), anti-Ogdh (ab137773, Abcam, 1:5000), anti-Suclg2 (ab187996, Abcam, 1:5000), anti-Sdha1 (ab139181, Abcam, 1:2000), anti-Fh (ab95947, Abcam, 1:2000), anti-Mdh2 (ab96193, Abcam, 1:1000), anti-Pcca (A304-324A, Bethyl, 1:5000), anti-Vdac1 (ab15895, Abcam, 1:2000). Anti-Pccb (1:4000) and anti-Mut (1:5000), were made by Bio-Synthesis, Lewisville, TX, USA against peptides containing amino acids NH2-CRLRATFAGLYSSLDVGEEGDQ-OH for Pccb and NH2-CPEWAALAKKQLKGKNPED-OH for Mut. Chicken anti-Rabbit IgG-HRP (sc-2955, Santa Cruz, 1:2000) was used as *se*condary antibody. Protein quantification was performed by measuring the amount of absorbance on a ChemiDoc™ MP Imaging System (170–8280; Bio-Rad) using Image Lab Software 5.1 by BioRad.

All immunoblot normalizations were performed using Vdac1, a mitochondrial membrane voltage dependent anion channel which is independent of the propionate and TCA cycle pathways, as loading control.

Enzyme rates calculation:

$$\text{Enzyme rate} = \text{Unit/(m)g protein} = \mu\text{mol} * \text{min}^{-1} * \text{(m)g} - {}^{1}$$

The slope of the measured analyte on the spectrophotometer is equal to the rate of the conversion (measured in units * sec^{-1}) and so slope *(60 s) * min^{-1} * mg^{-1} = slope (60) * min^{-1} *(amount of mitochondrial protein or total protein used for assay = mg^{-1}) is equal to the enzyme rate. All enzymatic figures use enzyme rate measured as pmol * sec^{-1} in which the amount of protein used is the amount of protein measured in mitochondrial lysate.

2.13. RNA isolation and expression profiling

RNA was isolated from two additional livers from each of the *Mut*-ko/ki and Ctl mice using the mirVANA isolation kit (Ambion, Life technologies) following manufacturer's instructions. RNA was analyzed for quality by electrophenogram and Northern blot prior to use to confirm that the RNA was of good quality as is standard in our institution. Expression was determined using the Clariom S mouse Array (Applied Biosystems). Fold change, *p*-values (with Bonferroni correction) and FDR *p* values were determined for 29, 129 probes. Data are all loaded under GEO number: GSE121060.

2.14. Statistics

All enzyme assays were done in triplicates in livers isolated from three separate animals (3 from *Mut*-ki/ko and 3 from Ctl animals). Means and standard deviations were calculated for all assays. Student *t*-tests were used to determine statistical significance ($p < .05$). Linear regression was done to evaluate the ratio of enyzme activity versus the normalized quantity of enzyme detected by immunoblot. Calculations were performed using GraphPad Prism v8.

3. Results

Here, we set out to define the effect of loss of Mmut on TCA cycle proteins/function. We used flash frozen liver taken from mice with a defect in methylmalonyl-CoA mutase (*Mut*-ko/ki, MMA) and compared them to littermate controls (ki/wt, Ctl).

Table 1
Amounts measured by Clariom S mouse Array (Applied Biosystems) of mRNA listed in the order of significance by *p*-value. Fold change (Log2) is also listed for each of the enzymes including Mmut, Fh, Idh2, Mdh2, Sdha, Cs, Ogdh, Suclg2, Vdac1.

Gene symbol	Mut-ki/ko Avg (log2)	Ctl Avg (log2)	Fold change	P-val
Mmut	6.59 ± 0.37	9.48 ± 1.37	−7.41	0.0119*
Fh	11.27 ± 0.32	10.22 ± 0.03	2.07	0.0138*
Idh2	10.36 ± 0.4	9.51 ± 0.15	1.79	0.0419*
Mdh2	7.81 ± 0.76	9.01 ± 0.97	−2.3	0.1196
Sdha	7.22 ± 0.82	7.77 ± 0.01	−1.47	0.2771
Cs	10.29 ± 0.59	10.54 ± 0.47	−1.19	0.5829
Ogdh	9.14 ± 0.76	8.91 ± 0.15	1.17	0.6206
Suclg2	9.82 ± 0.42	9.91 ± 0.66	−1.06	0.8477
Vdac1	9.84 ± 0.54	9.88 ± 0.82	−1.03	0.9402

* p value < .05.

To look at whether quantity of enzyme impacted activity, we measured levels of mRNA by microarray and protein amounts by immunoblot. Tables 1 and 2 summarize the mRNA expression results listing fold changes, Average log2 levels (Avg log2) and *p*-values for Ctl liver samples (Avg log2) and the *Mut*-ko/ki model (*Mut*-ko/ki Avg log2). Table 2 also lists the calculated amount of mRNA detected based on the standard Log2 average levels as reported standardly as mRNA quantification from microarrays seen in Table 1. Briefly, the *Mut*-ko/ki and Ctl had differences of expression of two-fold or more for Fh, Mdh2 and Mmut. More specifically, the *Mut*-ko/ki compared to the Ctl had 2.07-fold more Fh mRNA detected with a *p* value of 0.014. On the other hand, the liver from Ctl sample had 2.3-fold increased expression in Mdh2 than the *Mut*-ko/ki, but this difference does not meet the criteria for a significant p value. Mmut mRNA is significantly different in the *Mut*-ko/ki mouse compared to Ctl as is expected given its genotype with a fold change of −7.41. All other enzymes do not have fold changes greater than (or less than) 2 as well as non-significant *p* values.

To determine whether these differences correlate with protein amounts, we used semi-quantitative immunoblotting as measured by the Chemdoc system of each TCA cycle protein. Isolated mitochondria protein levels of Fh ($p = .024$), Mdh2 ($p = .029$), Ogdh (p = .02) and Mmut ($p = .003$) were significantly decreased in the MMA model compared to littermate controls (immunoblots in Fig. 2 and quantitation in Table 2).

Next, we measured the activity of individual TCA cycle enzymes from isolated, partially opened mitochondria. The enzymatic activity levels of individual TCA members were consistent with protein levels, whereby activity of Ogdhc was decreased, while there was a trend to a decrease for Fh and Mdh2 in the *Mut*-ko/ki mice while all others were similar to Ctl (Fig. 3, Suppl. Fig. S1–7).

Ogdhc activity is significantly decreased in the *Mut*-ko/ki mice compared to Ctl mice (student *t*-test, $p = .037$) as was the amount of protein ($p = .02$) (Figs. 2, 3, Suppl. Fig. S3, and Table 2). There is no difference in the RNA quantification for *Ogdh* of this enzyme (Tables 1 and 2). Unlike Ogdhc, Fh has a lower amount of enzyme activity (Fig. 3 and Table 2), but this does not reach statistical significance ($p = .11$) despite its lower enzyme amounts. There is a similar finding for Mdh2 (Fig. 3 and Table 2). Although activity appears decreased as well as enzyme amount, neither reach statistical significance. The differences between the *Mut*-ko/ki mouse model and Ctl appear to be correlated such that the amount of enzyme activity is consistent with the amount of enzyme observed for any one particular TCA component (Suppl. Fig. S8). Thus, even when the same amount of mitochondrial protein is used (whether for immunoblot or enzyme activity studies) the percentages of the amount of enzyme present in the whole extract differs between the *Mut*-ko/ki mouse model and the Ctl and the activity is consistent with that amount of enzyme.

Finally, since Mmut forms an anaplerotic reaction which feeds into the TCA cycle at succinate synthase (Ss), we further performed a multistep analysis, whereby we incubated mitochondria with methylmalonyl-CoA and examined production of fumarate, requiring the activities of Mmut, Ss, and Sdh. We found a significant decrease in this pathway activity in the *Mut*-ko/ki mice compared to Ctl ($p = .017$, Suppl, Fig. 9 and 10). This is the expected result given the deficiency of Mmut in this model and supports its utility as a model for MMA.

Our results suggest that in this model, there is decreased TCA cycle function. However, in our hands, this decreased function stems from decreased protein levels of certain TCA cycle proteins. We interpret our data to show that decreased protein levels come via regulation at the protein level, since mRNA abundance in MMA mice and littermate controls do not always correlate with protein amounts. Thus, we propose based on this data that loss of Mmut disrupts the TCA metabolon, resulting in loss of certain TCA cycle proteins and ultimately TCA cycle disruption.

4. Discussion

Here our interpretation of the evidence says that we can 1) assay the TCA cycle enzymes in samples prepared from flash frozen liver from mice (Ctl and *Mut*-ko/ki) and 2) demonstrate statistical differences in

Table 2
Comparison of quantitation of mRNA, protein, and enzyme activity identified for the TCA enzymes measured and Mmut in the *Mut*-ko/ki and the Ctl mouse liver samples. In general, protein levels appear to better correlate to enzyme activity than mRNA amounts.

Enzyme	Mut-ki/ko mRNA (Avg log2) levels	Ki/wt mRNA (Avg log2) levels	Mut- ko/ki ratio with Ki/wt mRNA ratio	Mut-ki/ko Protein (Amt/Amt Vdac1)	Ki/wt Protein (Amt/Amt Vdac1)	Mut- ko/ki ratio with Ki/wt Protein ratio	Mut- ko/ki Enzyme (nmol* s^{-1} * mg^{-1})	Ki/wt Enzyme nmol* s^{-1} * mg^{-1})	Mut-ko/ki ratio with Ki/wt Enzyme ratio
CS	10.29 ± 0.59	10.54 ± 0.47	0.97	0.96 ± 0.18	1.0 ± 0.12	0.95	68	62	1.1
IDH2(3) (Idh2)	10.36 ± 0.4	9.51 ± 0.15	1.09	0.75 ± 0.15	1.02 ± 0.22	0.74	43	50	0.87
OGDHc (Ogdh)	9.14 ± 0.76	8.91 ± 0.15	1.03	0.58*	1.01	0.57	1.2*	1.7	0.67
SCS (Suclg2)	9.82 ± 0.42	9.91 ± 0.66	0.99	0.95	1.01	0.93	140	130	1.1
SDH (Sdha)	7.22 ± 0.82	7.77 ± 0.01	0.92	0.7	1.04	0.67	15	16	0.91
Fh	11.27 ± 0.32	10.22 ± 0.03	1.1	0.57*	1	0.57	7.8	12	0.67
MDH2	7.81 ± 0.76	9.01 ± 0.97	0.86	0.66*	1	0.66	190	250	0.75
Mut (via SS-SDH)	6.59 ± 0.37	9.48 ± 1.37	0.69	0.49**	1	0.49	0.293	1.033	0.28

* $p < .05$.
** $p < .01$.

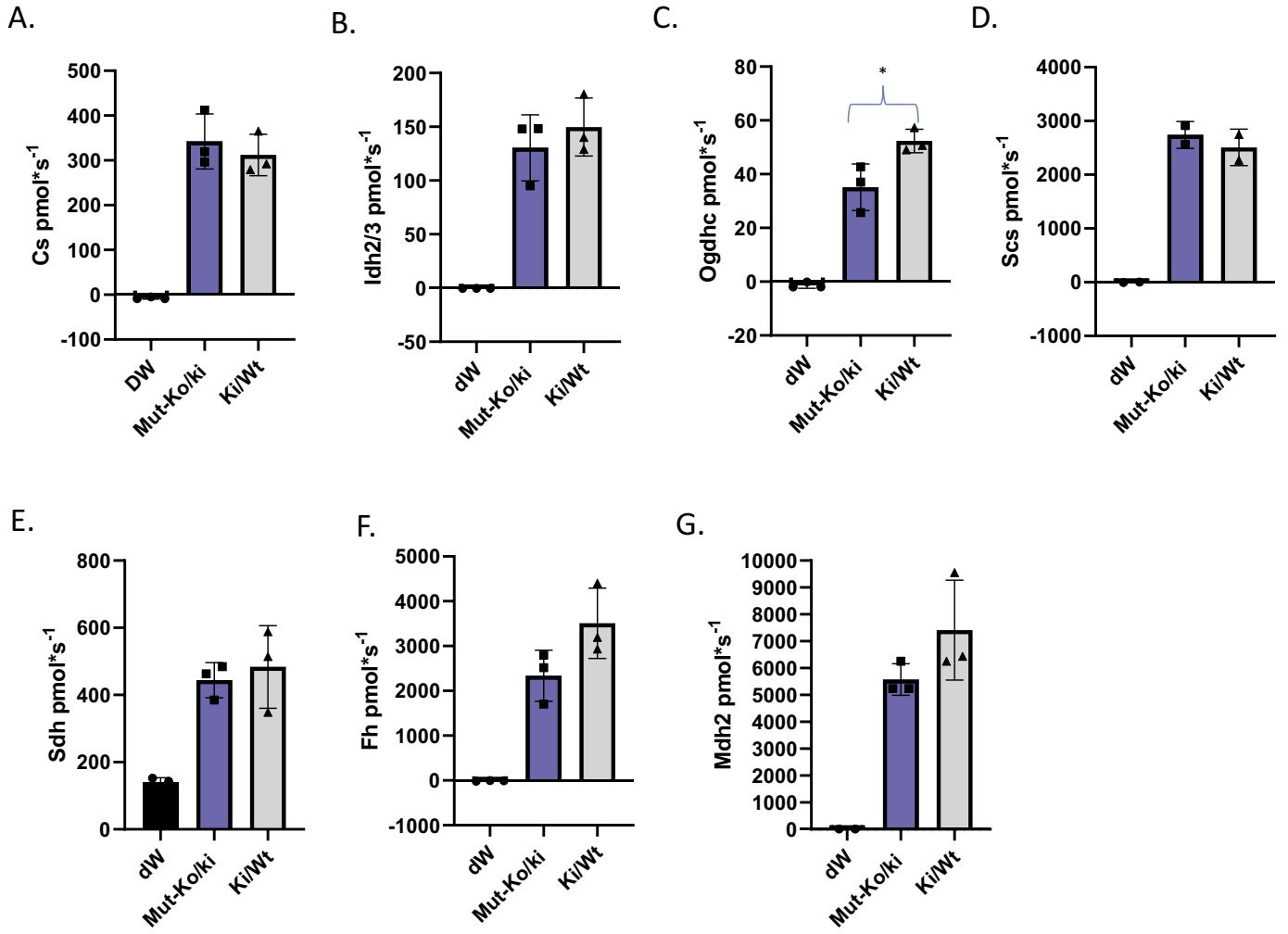

Fig. 3. Enzyme activity measured for each of the TCA enzymes assayed. For each graph, the experimental control (distilled water or dW, black, added instead of substrate), *Mut*-ko/ki (blue) and Ki/wt (grey) are listed. A. Cs activity (pmol/s per 5 μg mitochondrial protein), B. Idh2/3 activity (pmol/s per 30 μg mitochondrial protein), C. Ogdh activity (pmol/s per 30 μg mitochondrial protein). D. Succinyl-CoA synthetase activity (pmol/s per 20 μg mitochondrial protein), E. Sdh activity (pmol/s per 30 μg mitochondrial protein), F. Fh activity (pmol/s per 30 μg mitochondrial protein), H. Mdh2 activity (pmol/s per 30 μg mitochondrial protein). * $p < .05$. (For interpretation of the references to colour in this figure legend, the reader is referred to the web version of this article.)

enzyme activity between that of the *Mut*-ko/ki mouse and Ctl for Ogdhc which appears to be explained by amount of enzyme available. We observed no statistical differences in the quantity of most TCA enzyme (excluding Ogdh, Mdh2, and Fh) in the *Mut*-ko/ki and Ctl samples. In our hands, Ogdh, Fh, and Mdh2 show significant differences in quantity in the *Mut*-ko/ki mouse and Ogdhc also shows this in measured enzymatic rate. Increased statistical power from a larger number of samples may have allowed demonstration of a significant decrease in Fh and Mdh2 activity as well, since the difference in the amount of protein was small and the difference in activity would be expected to be small as well.

MMA's long-term complications are hypothesized to be a result of the accumulation of toxic intermediates (e.g. propionyl-CoA, methylmalonyl-CoA, 3-hydroxypropionate and 2-methycitrate, among others) which lead to abnormalities in enzyme functions resulting in decreased activity. The TCA dehydrogenases are a particularly concerning direct target [10,36–38]. In our study, we note some variation in enzyme function, but this variation correlates with the amount of enzyme observed (Fig. 2, Fig. 3, and Table 2). Here we see decreased OGDH activity and amounts, this could greatly impact the turnover in the TCA cycle since OGDH is a known regulator as well as would be a chokepoint.

Several studies have implicated the toxic intermediates from dysfunctional Mmut causing dehydrogenase dysfunction [10,19,39]. The *Mut*-ko/ki mice used here have elevated markers of disease include methylmalonate and propionylcarnitine to acetylcarnitine ratios which are associated with elevated propionyl-CoA [26] and so we expect that if such an inhibition of enzyme activity could be observed, we should have been able to detect it in this model. In our samples, the dehydrogenases (Ogdh, Idh2/3, Mdh2, and Sdh) do not have greater inhibition in the *Mut*-ko/ki mouse samples than other enzymes in the TCA cycle when activity is corrected for enzyme availability (Suppl. Fig.S8). This provides evidence against the toxic inhibitor hypothesis. However, it does not address whether amount of enzyme available for function is impacted by these toxins or whether higher amounts of these toxins would change this result.

There are some limitations to our study. Of note, we choose to not establish the aconitase assay since its iron-sulfur complex becomes dissociated with freezing [40] and felt that this assay was less informative at baseline. We acknowledge that these are flash frozen samples whereas fresh samples may potentially be better for assays since they are less likely to be impacted by freezing, but the goal was to demonstrate activity using this model so that other samples (e.g. human flash-frozen liver samples) which are not typically available in fresh states can be analyzed.

We recognize that fasting versus fed state can impact TCA enzyme

activity, but here we harvested the organisms from Ctl and *Mut*-ko/ki mice at the same time under the same conditions (fed state). Further studies are necessary to explore differences in quantitation under different conditions. There were no differences detected between female and male mice for enzyme activity in preliminary studies, here all are female mice.

In this paper, we have assayed TCA enzymes from flash frozen material from Ctl and *Mut*-ko/ki livers proving that this can be done on other flash frozen samples. We observed that TCA enzyme activity does vary for some enzymes, but this variation correlates with enzyme quantity. Finally, for Ogdh, the enzyme with the most different activity between the *Mut*-ko/ki and Ctl tissues, we have demonstrated that the protein quantitation differences are not reflected in the level of transcription. This suggests either changes in post-transcriptional processing or increased degradation of enzyme. Other enzymes in our study have differences at the level of transcription which reflect in differences in protein amounts.

These studies help clarify how complicated TCA cycle regulation is with differing levels of enzymes from the same amount of mitochondrial protein in the extract. This impacts the development of therapies for MMA, since the decreases in key elements of energy production may affect efforts at anaplerotic manipulation. These studies support the observation that MMA is a complex enzymatic phenotype with both upstream and downstream consequences.

Supplementary data to this article can be found online at https://doi.org/10.1016/j.ymgme.2019.10.007.

Acknowledgments

We would like to thank NIDDK for their gracious support through a K08DK105233 grant to Chapman. We would also like to thank Dr. Seth Berger who assisted with the gene expression analysis. The authors would also like to thank all our patients and all those families who participate in the Children's National Health Systems Genetics and Metabolism Bio-repository and who teach us about their diseases every day.

References

[1] W.A. Fenton, Branched-chain organic acidurias/acidemias, in: J. Fernandez, J.M. Saudubray, G. van den Berghe, J.H. Walter (Eds.), Inborn Metabolic Diseases, Springer, Wurzburg, Germany, 2006.
[2] I. Manoli, C.P. Venditti, Methylmalonic Acidemia, (1993).
[3] M.R. Baumgartner, F. Horster, C. Dionisi-Vici, G. Haliloglu, D. Karall, K.A. Chapman, M. Huemer, M. Hochuli, M. Assoun, D. Ballhausen, A. Burlina, B. Fowler, S.C. Grunert, S. Grunewald, T. Honzik, B. Merinero, C. Perez-Cerda, S. Scholl-Burgi, F. Skovby, F. Wijburg, A. MacDonald, D. Martinelli, J.O. Sass, V. Valayannopoulos, A. Chakrapani, Proposed guidelines for the diagnosis and management of methylmalonic and propionic acidemia, Orphanet J. Rare Dis. 9 (2014) 130.
[4] S. Kolker, V. Valayannopoulos, A.B. Burlina, J. Sykut-Cegielska, F.A. Wijburg, E.L. Teles, J. Zeman, C. Dionisi-Vici, I. Baric, D. Karall, J.B. Arnoux, P. Avram, M.R. Baumgartner, J. Blasco-Alonso, S.P. Boy, M.B. Rasmussen, P. Burgard, B. Chabrol, A. Chakrapani, K. Chapman, I.S.E. Cortes, M.L. Couce, L. de Meirleir, D. Dobbelaere, F. Furlan, F. Gleich, M.J. Gonzalez, W. Gradowska, S. Grunewald, T. Honzik, F. Horster, H. Ioannou, A. Jalan, J. Haberle, G. Haege, E. Langereis, P. de Lonlay, D. Martinelli, S. Matsumoto, C. Muhlhausen, E. Murphy, H.O. de Baulny, C. Ortez, C.C. Pedron, G. Pintos-Morell, L. Pena-Quintana, D.P. Ramadza, E. Rodrigues, S. Scholl-Burgi, E. Sokal, M.L. Summar, N. Thompson, R. Vara, I.V. Pinera, J.H. Walter, M. Williams, A.M. Lund, A. Garcia Cazorla, The phenotypic spectrum of organic acidurias and urea cycle disorders. Part 2: the evolving clinical phenotype, J. Inherit. Metab. Dis. 38 (2015) 1157–1158.
[5] C. Dionisi-Vici, F. Deodato, W. Roschinger, W. Rhead, B. Wilcken, 'Classical' organic acidurias, propionic aciduria, methylmalonic aciduria and isovaleric aciduria: long-term outcome and effects of expanded newborn screening using tandem mass spectrometry, J.Inherit.Metab Dis. 29 (2006) 383–389.
[6] M. Nizon, C. Ottolenghi, V. Valayannopoulos, J.B. Arnoux, V. Barbier, F. Habarou, I. Desguerre, N. Boddaert, J.P. Bonnefont, C. Acquaviva, J.F. Benoist, D. Rabier, G. Touati, P. de Lonlay, Long-term neurological outcome of a cohort of 80 patients with classical organic acidurias, Orphanet J. Rare Dis. 8 (2013) 148.
[7] F. Horster, M.R. Baumgartner, C. Viardot, T. Suormala, P. Burgard, B. Fowler, G.F. Hoffmann, S.F. Garbade, S. Kolker, E.R. Baumgartner, Long-term outcome in methylmalonic acidurias is influenced by the underlying defect (mut0, mut-, cblA, cblB), Pediatr. Res. 62 (2007) 225–230.
[8] S. Kolker, A.G. Cazorla, V. Valayannopoulos, A.M. Lund, A.B. Burlina, J. Sykut-Cegielska, F.A. Wijburg, E.L. Teles, J. Zeman, C. Dionisi-Vici, I. Baric, D. Karall, P. Augoustides-Savvopoulou, L. Aksglaede, J.B. Arnoux, P. Avram, M.R. Baumgartner, J. Blasco-Alonso, B. Chabrol, A. Chakrapani, K. Chapman, I.S. EC, M.L. Couce, L. de Meirleir, D. Dobbelaere, V. Dvorakova, F. Furlan, F. Gleich, W. Gradowska, S. Grunewald, A. Jalan, J. Haberle, G. Haege, R. Lachmann, A. Laemmle, E. Langereis, P. de Lonlay, D. Martinelli, S. Matsumoto, C. Muhlhausen, H.O. de Baulny, C. Ortez, L. Pena-Quintana, D.P. Ramadza, E. Rodrigues, S. Scholl-Burgi, E. Sokal, C. Staufner, M.L. Summar, N. Thompson, R. Vara, I.V. Pinera, J.H. Walter, M. Williams, P. Burgard, The phenotypic spectrum of organic acidurias and urea cycle disorders. Part 1: the initial presentation, J. Inherit. Metab. Dis. 38 (2015) 1041–1057.
[9] J.H. Walter, A. Michalski, W.M. Wilson, J.V. Leonard, T.M. Barratt, M.J. Dillon, Chronic renal failure in methylmalonic acidaemia, Eur. J. Pediatr. 148 (1989) 344–348.
[10] M.A. Schwab, S.W. Sauer, J.G. Okun, L.G. Nijtmans, R.J. Rodenburg, L.P. van den Heuvel, S. Drose, U. Brandt, G.F. Hoffmann, L.H. Ter, S. Kolker, J.A. Smeitink, Secondary mitochondrial dysfunction in propionic aciduria: a pathogenic role for endogenous mitochondrial toxins, Biochem.J. 398 (2006) 107–112.
[11] Y. de Keyzer, V. Valayannopoulos, J.F. Benoist, F. Batteux, F. Lacaille, L. Hubert, D. Chretien, B. Chadefeaux-Vekemans, P. Niaudet, G. Touati, A. Munnich, P. de Lonlay, Multiple OXPHOS deficiency in the liver, kidney, heart, and skeletal muscle of patients with methylmalonic aciduria and propionic aciduria, Pediatr.Res. 66 (2009) 91–95.
[12] L. Gallego-Villar, A. Rivera-Barahona, C. Cuevas-Martin, A. Guenzel, B. Perez, M.A. Barry, M.P. Murphy, A. Logan, A. Gonzalez-Quintana, M.A. Martin, S. Medina, A. Gil-Izquierdo, J.M. Cuezva, E. Richard, L.R. Desviat, In vivo evidence of mitochondrial dysfunction and altered redox homeostasis in a genetic mouse model of propionic acidemia: implications for the pathophysiology of this disorder, Free Radic. Biol. Med. 96 (2016) 1–12.
[13] S. Scholl-Burgi, J.O. Sass, J. Zschocke, D. Karall, Amino acid metabolism in patients with propionic acidaemia, J. Inherit. Metab. Dis. 35 (2010) 65–70.
[14] H.R. Filipowicz, S.L. Ernst, C.L. Ashurst, M. Pasquali, N. Longo, Metabolic changes associated with hyperammonemia in patients with propionic acidemia, Mol. Genet. Metab. 88 (2006) 123–130.
[15] I. Manoli, J.R. Sysol, L. Li, P. Houillier, C. Garone, C. Wang, P.M. Zerfas, K. Cusmano-Ozog, S. Young, N.S. Trivedi, J. Cheng, J.L. Sloan, R.J. Chandler, M. Abu-Asab, M. Tsokos, A.G. Elkahloun, S. Rosen, G.M. Enns, G.T. Berry, V. Hoffmann, S. DiMauro, J. Schnermann, C.P. Venditti, Targeting proximal tubule mitochondrial dysfunction attenuates the renal disease of methylmalonic acidemia, Proc.Natl.Acad.Sci.U.S.A 110 (2013) 13552–13557.
[16] K.R. Atkuri, T.M. Cowan, T. Kwan, A. Ng, L.A. Herzenberg, L.A. Herzenberg, G.M. Enns, Inherited disorders affecting mitochondrial function are associated with glutathione deficiency and hypocitrullinemia, Proc. Natl. Acad. Sci. U. S. A. 106 (2009) 3941–3945.
[17] J.M. Saudubray, F. Sedel, J.H. Walter, Clinical approach to treatable inborn metabolic diseases: an introduction, J.Inherit.Metab Dis. 29 (2006) 261–274.
[18] F.X. Coude, L. Sweetman, W.L. Nyhan, Inhibition by propionyl-coenzyme A of N-acetylglutamate synthetase in rat liver mitochondria. A possible explanation for hyperammonemia in propionic and methylmalonic acidemia, J.Clin.Invest 64 (1979) 1544–1551.
[19] A.M. Brusque, C.F. Mello, D.N. Buchanan, S.T. Terracciano, M.P. Rocha, C.R. Vargas, C.M. Wannmacher, M. Wajner, Effect of chemically induced propionic acidemia on neurobehavioral development of rats, Pharmacol.Biochem.Behav. 64 (1999) 529–534.
[20] N. Longo, L.B. Price, E. Gappmaier, N.L. Cantor, S.L. Ernst, C. Bailey, M. Pasquali, Anaplerotic therapy in propionic acidemia, Mol. Genet. Metab. 122 (2017) 51–59.
[21] O.E. Owen, S.C. Kalhan, R.W. Hanson, The key role of anaplerosis and cataplerosis for citric acid cycle function, J. Biol. Chem. 277 (2002) 30409–30412.
[22] P.A. Srere, B. Sumegi, A.D. Sherry, Organizational aspects of the citric acid cycle, Biochem.Soc.Symp. 54 (1987) 173–178.
[23] Y. Zhang, K.F.M. Beard, C. Swart, S. Bergmann, I. Krahnert, Z. Nikoloski, A. Graf, R.G. Ratcliffe, L.J. Sweetlove, A.R. Fernie, T. Obata, Protein-protein interactions and metabolite channelling in the plant tricarboxylic acid cycle, Nat. Commun. 8 (2017) 15212.
[24] F.M. Meyer, J. Gerwig, E. Hammer, C. Herzberg, F.M. Commichau, U. Volker, J. Stulke, Physical interactions between tricarboxylic acid cycle enzymes in Bacillus subtilis: evidence for a metabolon, Metab. Eng. 13 (2011) 18–27.
[25] M.M. Islam, M. Nautiyal, R.M. Wynn, J.A. Mobley, D.T. Chuang, S.M. Hutson, Branched-chain amino acid metabolon: interaction of glutamate dehydrogenase with the mitochondrial branched-chain aminotransferase (BCATm), J. Biol. Chem. 285 (2010) 265–276.
[26] P. Forny, A. Schumann, M. Mustedanagic, D. Mathis, M.A. Wulf, N. Nagele, C.D. Langhans, A. Zhakupova, J. Heeren, L. Scheja, R. Fingerhut, H.L. Peters, T. Hornemann, B. Thony, S. Kolker, P. Burda, D.S. Froese, O. Devuyst, M.R. Baumgartner, Novel mouse models of methylmalonic aciduria recapitulate phenotypic traits with a genetic dosage effect, J. Biol. Chem. 291 (2016) 20563–20573.
[27] H. Peters, M. Nefedov, J. Sarsero, J. Pitt, K.J. Fowler, S. Gazeas, S.G. Kahler, P.A. Ioannou, A knock-out mouse model for methylmalonic aciduria resulting in neonatal lethality, J. Biol. Chem. 278 (2003) 52909–52913.
[28] D. Shepherd, P.B. Garland, The kinetic properties of citrate synthase from rat liver mitochondria, The Biochem. J. 114 (1969) 597–610.
[29] C. Bai, E. Fernandez, H. Yang, R. Chen, Purification and stabilization of a monomeric isocitrate dehydrogenase from Corynebacterium glutamicum, Protein Expr. Purif. 15 (1999) 344–348.

[30] G.E. Gibson, K.F. Sheu, J.P. Blass, A. Baker, K.C. Carlson, B. Harding, P. Perrino, Reduced activities of thiamine-dependent enzymes in the brains and peripheral tissues of patients with Alzheimer's disease, Arch. Neurol. 45 (1988) 836–840.
[31] S. Goncalves, V. Paupe, E.P. Dassa, J.J. Briere, J. Favier, A.P. Gimenez-Roqueplo, P. Benit, P. Rustin, Rapid determination of tricarboxylic acid cycle enzyme activities in biological samples, BMC Biochem. 11 (2010) 5.
[32] C. Veeger, D.V. DerVartanian, W.P. Zeylemaker, [16] Succinate dehydrogenase: [EC 1.3.99.1 Succinate: (acceptor) oxidoreductase], Methods in Enzymology, Academic Press, 1969, pp. 81–90.
[33] R.A. Bradshaw, G.W. Robinson, G.M. Hass, R.L. Hill, The reaction of fumarase with iodoacetate and 4-bromocrotonate, J. Biol. Chem. 244 (1969) 1755–1763.
[34] G.B. Kitto, Purification and properties of ostrich heart malate dehydrogenases, Biochim. Biophys. Acta 139 (1967) 16–23.
[35] S. Taoka, R. Padmakumar, M.T. Lai, H.W. Liu, R. Banerjee, Inhibition of the human methylmalonyl-CoA mutase by various CoA-esters, J. Biol. Chem. 269 (1994) 31630–31634.
[36] N. Gregersen, The specific inhibition of the pyruvate dehydrogenase complex from pig kidney by propionyl-CoA and isovaleryl-co-a, Biochem. Med. 26 (1981) 20–27.
[37] D.A. Stumpf, J. McAfee, J.K. Parks, L. Eguren, Propionate inhibition of succinate:CoA ligase (GDP) and the citric acid cycle in mitochondria, Pediatr. Res. 14 (1980) 1127–1131.
[38] J.C. Dutra, C.S. Dutra-Filho, S.E. Cardozo, C.M. Wannmacher, J.J. Sarkis, M. Wajner, Inhibition of succinate dehydrogenase and beta-hydroxybutyrate dehydrogenase activities by methylmalonate in brain and liver of developing rats, J. Inherit. Metab. Dis. 16 (1993) 147–153.
[39] D.R. Melo, S.R. Mirandola, N.A. Assuncao, R.F. Castilho, Methylmalonate impairs mitochondrial respiration supported by NADH-linked substrates: involvement of mitochondrial glutamate metabolism, J. Neurosci. Res. 90 (2012) 1190–1199.
[40] F.J. Ruzicka, H. Beinert, The soluble "high potential" type iron-sulfur protein from mitochondria is aconitase, J. Biol. Chem. 253 (1978) 2514–2517.